

Pion form factor using domain wall valence and `asqtad` sea quarks

G. T. Fleming^{ab}, F. D. R. Bonnet^{ac}, R. G. Edwards^a, R. Lewis^c and D. G. Richards^a

^a Thomas Jefferson National Accelerator Facility, Newport News, VA 23606, USA.

^b Sloane Physics Laboratory, Yale University, New Haven, CT, 06520, USA

^c Department of Physics, University of Regina, Regina, SK, S4S 0A2, Canada.

We compute the pion electromagnetic form factor in a hybrid calculation with domain wall valence quarks and improved staggered (`asqtad`) sea quarks. This method can easily be extended to $\rho \rightarrow \gamma\pi$ transition form factors.

The pion electromagnetic form factor is considered a good observable for studying the onset with increasing energy of the perturbative QCD regime for exclusive processes. As the pion is the lightest and simplest hadron, a perturbative description is believed to be valid at lower energy scales than predictions for heavier and more complicated hadrons like the nucleon [1].

A pseudoscalar particle has only a single electromagnetic form factor, $F(Q^2)$, where Q^2 is the four-momentum transfer, and at $Q^2 = 0$, this form factor is the electric charge of the particle, $F(Q^2 = 0) = 1$; the magnetic form factor vanishes. The experimentally observed behavior of the form factor at small momentum transfer is well described by the vector meson dominance (VMD) hypothesis [2,3,4]

$$F_\pi(Q^2) \approx \frac{1}{1 + Q^2/m_{\text{VMD}}^2} \quad \text{for } Q^2 \ll m_{\text{VMD}}^2 \quad (1)$$

The current experimental situation is presented in Fig. 1 [5,6,7,8,9].

What is surprising is that VMD with only the lightest resonance ($m_\rho = m_{\text{VMD}}$) appears to describe all the existing data, even up to scales of $Q^2 \gtrsim 1\text{GeV}^2$. In contrast, at very high momentum transfer, we expect the data to approach the perturbative behavior [10,11,12]

$$F_\pi(Q^2) = \frac{8\pi\alpha_s(Q^2)f_\pi^2}{Q^2} \quad \text{as } Q^2 \rightarrow \infty \quad (2)$$

Higher order perturbative calculations of the hard contribution to the form factor [13,14,15] do not

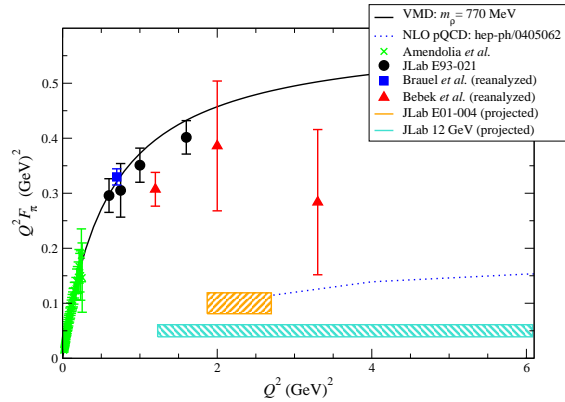


Figure 1. Summary of experimental data for the pion electromagnetic form factor. Shaded regions are expected sensitivities of future experiments.

vary significantly from this value, as seen in Fig. 1. At the largest energy scale where reliable experimental measurements have so far been obtained, around $Q^2 \simeq 2\text{GeV}^2$, the data are 100% larger than this pQCD asymptotic prediction.

Early lattice calculations validated the vector meson dominance hypothesis at low Q^2 [16, 17]. Recent lattice results [18,19,20,21], including some of our own preliminary results [22,23], have somewhat extended the range of momentum transfer, up to 2GeV^2 , and the results remain consistent with VMD and the experimental data.

For our exploration of the pion form factor with unquenched gauge configurations, we performed a hybrid calculation using MILC $N_f = 2 + 1$ and $N_f = 3$ configurations in $20^3 \times 64$ volumes,

Table 1

Simulation details for domain wall fermion calculations on $20^3 \times 64$ dynamical MILC `asqtad` lattices at $a^{-1} \approx 1.6$ GeV.

am_{ud}	am_s	am_{val}	m_ρ (MeV)	m_π (MeV)
0.01	0.05	0.01	956(22)	318(3)
0.05	0.05	0.05	955(19)	602(5)
0.05	0.05	0.081	1060(14)	758(5)

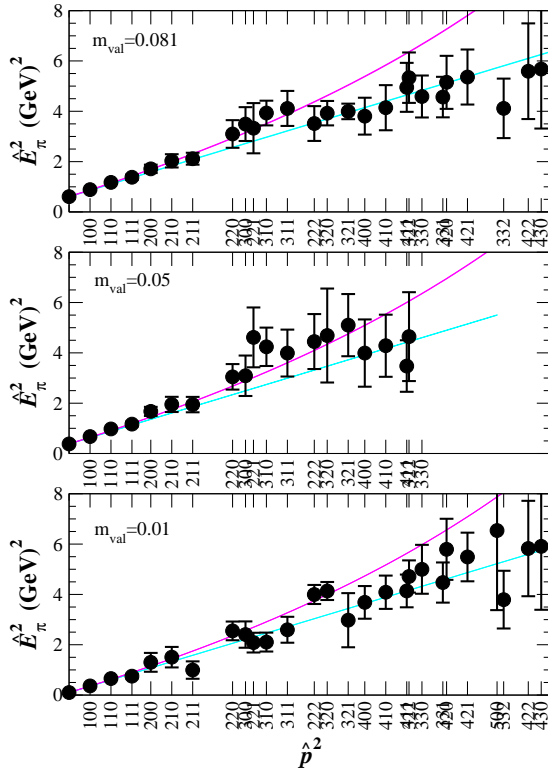


Figure 2. Pion (left) and rho meson (right) dispersion relation *vs.* continuum (upper) and lattice (lower) expectations curves.

generated with staggered `asqtad` sea quarks[24], and domain wall valence quarks with domain wall height $m_0 = 1.7$ and extent $L_s = 16$ of the extra dimension [25]. The MILC configurations were HYP blocked [26] before valence propagators were computed, otherwise the residual chiral symmetry breaking would have been unacceptably large. Dirichlet boundary conditions were imposed 32 timeslices apart. Thus, opposite halves of the lattices were used on alternate configurations in the Monte Carlo sequence in order to reduce autocorrelations. A detailed study of the physical properties of light hadrons composed of staggered quarks computed on these lattices has recently been completed[27]. Details of the observables we computed are available in our earlier references [22,23].

To compute the pion form factor at large momentum transfer, we must first understand the pion dispersion relation when the momenta are relatively large. In the continuum limit, we expect proper relativistic behaviour

$$E_\pi^2(\mathbf{p}) = \mathbf{p}^2 + E_\pi^2(0). \quad (3)$$

From the study of free lattice bosons, we can define lattice equivalents of the continuum momentum and energy

$$\hat{E} = 2 \sinh(E/2) \quad \hat{p}_x = 2 \sin(p_x/2). \quad (4)$$

Another possibility is that the pion dispersion relation will follow that of a free lattice boson

$$\hat{E}_\pi^2(\hat{\mathbf{p}}) = \hat{\mathbf{p}}^2 + \hat{E}_\pi^2(0) \quad (5)$$

Eqs. (3) and (5) differ significantly only when the lattice momenta are large.

In Fig. 2, we have plotted against each dispersion relation and we see that the data clearly favor the lattice dispersion relation at large momenta. This gives us confidence that we can use Eq. (5) to determine $E_\pi(\mathbf{p})$ at high momenta from fits to low momentum correlators which have much less statistical noise.

Using the lattice dispersion relation and the ratio method described in our previous work, we have computed in Fig. 3 the pion form factor for two dynamical pion masses. Fits of the data to the monopole form of Eq. (1) are also shown,

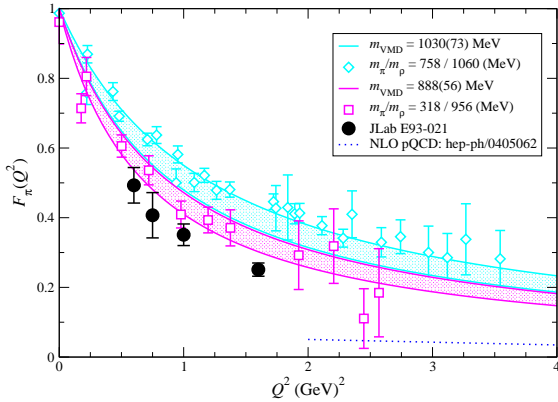


Figure 3. Pion electromagnetic form factor for fixed sink momentum $\mathbf{p}_f = (1, 0, 0)$ computed by the ratio method [22,23] and imposing the lattice dispersion relation, Eq. (5). Shaded regions are jackknife error bands for VMD fit.

where shaded regions correspond to jackknife error bands and the central values are given in the legend. The data in Fig. 3 were computed with pseudoscalar pion sink operator fixed at momentum $\mathbf{p}_f = (1, 0, 0)$. We were unable to compute statistically significant form factors with the same pseudoscalar sink operator for $\mathbf{p}_f = (1, 1, 0)$ by the ratio method, apparently due to the poor overlap of the sink operator with the higher momentum state. We expect that an axial vector sink operator would be a better choice for future calculations. A comparison of the ratio method with the fitting method, also described in [22,23], should appear shortly [28].

This work was supported in part by the Natural Sciences and Engineering Research Council of Canada and by the U.S. Department of Energy under contract DE-AC05-84ER40150. Computations were performed on the 128-node and 256-node Pentium IV clusters at JLab and on other resources at ORNL, under the auspices of the U.S. DoE's SciDAC initiative.

REFERENCES

1. N. Isgur and C.H. Llewellyn Smith, Phys. Rev. Lett. 52 (1984) 1080.
2. W.G. Holladay, Phys. Rev. 101 (1956) 1198.
3. W.R. Frazer and J.R. Fulco, Phys. Rev. Lett. 2 (1959) 365.
4. W.R. Frazer and J.R. Fulco, Phys. Rev. 117 (1960) 1609.
5. NA7, S.R. Amendolia et al., Nucl. Phys. B277 (1986) 168.
6. C.J. Bebek et al., Phys. Rev. D17 (1978) 1693.
7. P. Brauel et al., Zeit. Phys. C3 (1979) 101.
8. Jefferson Lab F_π , J. Volmer et al., Phys. Rev. Lett. 86 (2001) 1713, nucl-ex/0010009.
9. H.P. Blok, G.M. Huber and D.J. Mack, (2002), nucl-ex/0208011.
10. S.J. Brodsky and G.R. Farrar, Phys. Rev. Lett. 31 (1973) 1153.
11. S.J. Brodsky and G.R. Farrar, Phys. Rev. D11 (1975) 1309.
12. G.R. Farrar and D.R. Jackson, Phys. Rev. Lett. 43 (1979) 246.
13. N.G. Stefanis, W. Schroers and H.C. Kim, Phys. Lett. B449 (1999) 299, hep-ph/9807298.
14. N.G. Stefanis, W. Schroers and H.C. Kim, Eur. Phys. J. C18 (2000) 137, hep-ph/0005218.
15. A.P. Bakulev et al., (2004), hep-ph/0405062.
16. G. Martinelli and C.T. Sachrajda, Nucl. Phys. B306 (1988) 865.
17. T. Draper et al., Nucl. Phys. B318 (1989) 319.
18. J. van der Heide et al., Phys. Lett. B566 (2003) 131, hep-lat/0303006.
19. RBC, Y. Nemoto, (2003), hep-lat/0309173.
20. J. van der Heide, J.H. Koch and E. Laermann, Phys. Rev. D69 (2004) 094511, hep-lat/0312023.
21. A.M. Abdel-Rehim and R. Lewis, (2004), hep-lat/0408033.
22. LHPC, F.D.R. Bonnet et al., (2003), hep-lat/0310053.
23. LHPC, F.D.R. Bonnet et al., Nucl. Phys. Proc. Suppl. 128 (2004) 59, hep-lat/0312008.
24. C.W. Bernard et al., Phys. Rev. D64 (2001) 054506, hep-lat/0104002.
25. J.W. Negele et al., Nucl. Phys. Proc. Suppl. 128 (2004) 170, hep-lat/0404005.
26. A. Hasenfratz and F. Knechtli, Phys. Rev. D64 (2001) 034504, hep-lat/0103029.
27. C. Aubin et al., (2004), hep-lat/0402030.
28. LHPC, G.T. Fleming et al., In preparation.